A proteome-wide, MS-based screen identifies SUMOylation of host RNA splicing factors induced by HIV-1 infection

Demetra P. Kelenis[1], Jeffrey R. Johnson[2], Simone Sidoli[3], Ann Emery[4], Ronald Swanstrom[5], Luke J. Hawkins[1], Tegh Pawar[1], and Stephen P. Goff[1,6]

[1]Columbia University, Biochemistry and Molecular Biophysics, New York, [2]NY, Icahn School of Medicine at Mount Sinai, Microbiology, New York, NY, [3]Albert Einstein College of Medicine, Biochemistry, New York, NY, [4]University of North Carolina at Chapel Hill, Genetics and Molecular Biology, Chapel Hill, NC, [5]University of North Carolina at Chapel Hill, Biochemistry and Biophysics, Chapel Hill, NC, [6]Columbia University, Microbiology and Immunology, New York, NY

ABSTRACT

HIV-1 exploits host cell post-translation modifications (PTMs) to facilitate production of infectious particles. These modifications include SUMOylation, a dynamically regulated PTM involving covalent attachment of small ubiquitin-like modifiers (SUMOs) to lysine (K) residues of target proteins. SUMOylation modulates the activity of thousands of proteins and multiple fundamental host cellular processes, including pathways hijacked by HIV-1 to promote infection and spread. The SUMOylation of several proteins during HIV-1 infection has been characterized. However, the broad effects of HIV-1 infection on the SUMOylation of the host cell proteome is largely unknown. To date, SUMOylation has not been explored by large-scale proteomics in the context of HIV infection, where many SUMO-regulated host dependency factors remain to be identified. In this study, we performed a proteome-wide, mass spectrometry (MS)-based screen to identify proteins that are SUMOylated during HIV-1 infection. Here, and in immunoprecipitation assays, infection with HIV-1 led to the widespread increased SUMOylation of heterogeneous nuclear

ribonucleoprotein (HNRNP) A/B family members. We selected HNRNPA2B1 (A2/B1) and HNRNPA3 for further study. We find that infection with HIV-1 specifically induced the SUMOylation of both proteins by SUMO1 and SUMO2 paralogs in multiple biochemical assays and in multiple human cell lines. Current efforts include generating non-SUMOylatable HNRNPA2B1 and HNRNPA3 mutants to test the functional consequences of their SUMOylation on the splicing of HIV-1 mRNAs. Together, our data point to a novel mechanism involving HIV-1-induced SUMOylation of these host RNA splicing factors as a means to regulate HIV-1 splice variant production. Broadly, our findings suggest that infection with HIV-1 alters the SUMOylation of many unexplored host cellular proteins, and provides a proteomic resource for their future mechanistic study.

INTRODUCTION

SUMOylation is a reversible, dynamic post-translational modification (PTM) involving covalent attachment of Small Ubiquitin-like Modifier (SUMO) proteins to lysine (K) residues of substrate proteins. Like ubiquitination, SUMOylation occurs via a three-step, ATP-dependent enzymatic cascade including an E1 activating enzyme (SAE1/SAE2), E2 conjugase (UBC9), and for some substrates, an E3 ligase.[1,2,3] Unlike ubiquitination, SUMOylation does not typically target proteins for degradation and instead influences protein function, often by promoting non-covalent interactions with SUMO Interacting Motif (SIM)-containing cofactors. Conserved from yeast to mammals, SUMOylation modulates the activity of thousands of proteins and multiple fundamental cellular process.[4,5,6,7] SUMOylation also provides cells with a rapid, versatile mechanism to alter proteomic activity in response to various stimuli, including viral infection. In turn, both DNA and RNA viruses have been shown to manipulate host cell SUMOylation by directly targeting the SUMO pathway.[6,2,3,8]

Like other viruses, human immunodeficiency virus type 1 (HIV-1) is entirely dependent upon the host cell machinery for completion of the viral life cycle and is known to manipulate this

machinery to ensure infection and spread. HIV-1 directly exploits host PTMs including glycosylation, myristoylation, phosphorylation, ubiquitination, and SUMOylation to facilitate production of infectious particles.[9,10] SUMOylation of the HIV-1 viral proteins p6 and integrase (IN) has been reported, where SUMOylation of p6 was shown to compete with ubiquitination at the same residue and inhibit recruitment of ESCRT machinery during virus production, while SUMOylation of IN influences the integration efficiency of the HIV-1 DNA into the host cell genome.[11,12,13,14] SUMOylation of unintegrated chromatinized HIV-1 DNA has also been shown to mediate the establishment of HIV-1 latency.[15]

HIV-1 also appropriates multiple host cell pathways known to be regulated by SUMOylation, such as intracellular trafficking, nucleocytoplasmic transport, chromatin remodeling, transcription, and RNA processing, including alternative splicing.[3] For instance, alternative splicing of the HIV-1 primary transcript greatly expands the coding capacity of its ~9.2 kb viral genome, allows temporal regulation of HIV-1 gene expression, and is necessary for the expression of most HIV-1 viral proteins.[16,17,18,19] To produce these spliced transcripts, HIV-1 repurposes the host cell RNA splicing machinery, where SUMOylation of spliceosomal proteins is known to regulate spliceosome assembly in contexts outside HIV-1 infection.[20,21] Although the SUMOylation of several host proteins such as NFKBIA, LEDGF/p75 (PSIP1), and SAMHD1 have been shown to influence HIV-1 infection, these studies relied on targeted analysis of proteins already known to play a role in HIV-1 replication. The way in which HIV-1 alters the SUMOylation of host cell proteins on a large scale however is largely unexplored.[9,22,23,24,25] To date, SUMOylation has not been studied by system-wide proteomics in the context of HIV-1 infection, where many SUMO-regulated host dependency factors remain to be identified and the functional significance of these modifications explored.

In this study, we performed an unbiased, proteome-wide mass spectrometry (MS)-based screen to identify host cell proteins that are SUMOylated in response to HIV-1 infection in human cells. We selected 30 proteins from these data and experimentally validated the effects of HIV-1

infection on their SUMOylation status, where infection with HIV-1 led to widespread SUMOylation of heterogeneous nuclear ribonucleoprotein (HNRNP) A/B family members. We focused our attention on two of these proteins, HNRNPA2B1 (A2/B1) and HNRNPA3, which were found to be SUMOylated upon HIV-1 infection by both SUMO1 and SUMO2 paralogs across multiple cell line models. We are currently investigating the functional significance of HIV-1-induced SUMOylation of HNRNPA2B1 and HNRNPA3 using un-SUMOylatable mutants.

Taken together, our findings suggest a novel mechanism by which HIV-1-induced SUMOylation of HNRNPA2B1 and HNRNPA3 modulate their role in HIV-1 alternative splicing. More broadly, our results suggest that infection with HIV-1 alters the SUMOylation of a diverse set of unexplored host cell proteins, and provides a proteomic resource for future mechanistic study of these modifications' function.

RESULTS

Proteome-wide screen identifies HIV-1-induced SUMO substrates

The human genome encodes five SUMO paralogs (SUMO1-5). SUMO1-3 are expressed ubiquitously, while the expression of SUMO4 and 5 is restricted to specific tissues. SUMO2 and 3 are 97% identical in amino acid sequence and are often grouped together as SUMO2/3. SUMO1 and SUMO2/3 share only 47% sequence homology and are regarded as functionally distinct.[1,2,3] To investigate the dynamics of SUMOylation in response HIV-1 infection by the main SUMO paralogs, we utilized a previously described proteomic strategy[3,26] to identify host cell proteins that change in SUMO1 or SUMO2 modification status following infection with HIV-1.

We generated stable cell lines expressing SUMO1 or SUMO2 fused to an N-terminal 3xFLAG tag. To facilitate mapping by MS, our SUMO constructs also included previously described C-terminal glutamine to arginine (Q to R) mutations (3xFLAG-SUMO1^{Q92R}, 3xFLAG-SUMO2^{Q88R}). These mutations introduce a trypsin cleavage site near the C-terminus of SUMO, leaving a unique five amino acid remnant on the SUMO1 versus SUMO2-modified peptides

following tryptic digest (Figure 1A).[3,26] 3xFLAG-tagged SUMO1 and SUMO2 mutants were expressed at levels comparable to endogenous WT SUMOs, and were conjugated to target proteins in the respective cell lines (Supplemental Figure 1A). To enable comparison between different strategies for enriching SUMOylated substrates, we also generated cell lines stably expressing HIS_6-tagged $SUMO1^{Q92R}$ or $SUMO2^{Q88R}$ (Figure 1A). Both 3xFLAG and HIS_6-tagged $SUMO1^{Q92R}$ immunoprecipitated with RANGAP1, a well-characterized SUMO1 substrate (Supplemental Figure 1B).[27] This suggests that that the combinations of N-terminal tag and C-terminal mutations utilized did not interfere with conjugation of SUMO mutants to endogenous target proteins. HIV-1 infection efficiency and reporter expression was also unaffected in the 3xFLAG or HIS_6-tagged SUMO cell lines, indicating that expression of exogenous SUMOs did not interfere with HIV-1 infection (Supplemental Figure 1C).

The 3xFLAG- and HIS_6-tagged SUMO1 and SUMO2 cell lines were used to identify host proteins that change in SUMOylation status in response to HIV-1 infection. Cells were either left uninfected, or infected with single-cycle HIV-1 (pNL4-3 deltaENV-EGFP) and harvested at 24 hours post-infection (hpi). 3xFLAG-SUMO-conjugated proteins were isolated from cell lysates using an anti-FLAG antibody, while HIS_6-SUMO-conjugated proteins were enriched using a Nickel-NTA column. SUMO-conjugated proteins were isolated under denaturing conditions to dissociate non-covalent interactors and inactivate SUMO proteases. Proteins were trypsinized and analyzed by liquid chromatography–tandem mass spectrometry (LC-MS/MS) for protein identification and abundance quantification (Figure 1B).

This approach identified 3,717 total SUMO1-modified proteins and 3,749 SUMO2-modified proteins (Supplemental Table 1, Tabs A and B), in addition to a small number of -EQTGG (SUMO1) or -QQTGG (SUMO2)-modified peptides (Supplemental Table 2). These data included many proteins that were increased or decreased in the HIV-1-infected samples relative to the uninfected controls. We first compared the total list of SUMO-modified substrates identified in this study to a database of SUMOylated proteins comprised of data from 22 proteomic studies.[28] Here,

~54% of all SUMOylated proteins identified in our study overlapped with those previously reported in the database (Supplemental Figure 2A). Our data also included many well-known SUMO substrates such as RANGAP1, TOP2A, PML, SART1, SAFB2, RANBP2, PCNA, TRIM28, TRIM33, BLM, and BRCA1, as well as proteins whose SUMOylation status has been shown to modulate acute HIV-1 infection (NFKBIA, PSIP1, SAMHD1) or HIV-1 latency (PLK1, CDK9) (Supplemental Table 1, Tabs A and B).[9,22,23,24,25,29,30] Together, these findings support the validity of our approach for identifying confirmed SUMO substrates, and suggest that there are many unexplored proteins that may become SUMO1 or SUMO2 targets upon HIV-1 infection.

The effect of HIV-1 infection on all SUMO1- or SUMO2-modified substrates identified in the 3xFLAG- or HIS_6-tagged cell lines is shown in Figure 1C. The y-axis indicates the Log2 fold change in abundance of these proteins in the HIV-1-infected samples relative to the uninfected controls. On average, a slightly higher percentage of SUMO substrates were increased by HIV-1 infection (SUMOylated, 60%) versus decreased (deSUMOylated, 40%). For most of these proteins, infection with HIV-1 did not lead to a Log_2 dynamic range larger than 1 (2-fold linear change up or down). Still, 463 SUMO1 substrates and 244 SUMO2 substrates increased or decreased more than 2-fold with HIV-1 infection (Figure 1C) (Supplemental Table 1, Tabs C-F). Together, these findings suggest that HIV-1 infection leads to concomitant SUMOylation and deSUMOylation of different sets of host proteins, with HIV-1 substantially altering the SUMOylation status or abundance of many substrates. Comparison between SUMO1 versus SUMO2 substrates that were increased or decreased following HIV-1 infection, respectively, revealed a high degree of overlap (Figure 1D) (Supplemental Table 1, Tab G), suggesting that most of the SUMO substrates we identified can be modified be either SUMO1 or SUMO2 during HIV-1 infection.

HIV-1 infection leads to SUMOylation of HNRNPs and other splicing factors

To identify proteins that are consistently SUMOylated upon HIV-1 infection regardless of tag or enrichment strategy, we looked for substrates that had similar quantitative changes in SUMO1 or

SUMO2 modification in response to HIV-1 infection in both the 3xFLAG-tagged and HIS_6-tagged SUMO cell lines (Figure 1E, F) . Among the SUMO1 substrates identified in both the 3xFLAG- and HIS_6-tagged cell lines, there were numerous HNRNP family members that were increased following infection with HIV-1, including HNRNPs A2B1, A3, H1, H2, C, F, K, M, R, U, A0 and A1 (Figure 1E) (Supplemental Table 1, Tab H). Similarly, among the SUMO2 substrates identified in both the 3xFLAG- and HIS_6-tagged cell lines, HNRNPs A2B1, A3, A0, U, H2, H1, C, K, R, U, A1, and AB were enriched in the HIV-1 infected cells relative to the uninfected controls (Figure 1F) (Supplemental Table 1, Tab H). The shared SUMOylation of many these HNRNPs by both SUMO1 and SUMO2 upon HIV-1 infection is consistent with the high level of overlap in SUMO1 and SUMO2 substrates observed in our data (Figure 1D). Consistent with the role of HNRNPs in regulating multiple aspects of nucleic acid metabolism, including alternative splicing,[31] the HIV-1-induced SUMO1 and SUMO2 substrates were significantly enriched for Reactome pathways “Metabolism of RNA”, “mRNA splicing”, and “Processing of capped intron-containing pre-mRNA”, among other RNA-related pathways (Figure 1G, H) (Supplemental Table 1, Tab I). The HIV-1-induced SUMO substrates also included additional splicing factors such as SRSF6, TRA2B, PHF5A, CCAR1, and SRRM2. (Figure 1G, H). Importantly, western blot analysis of 30 of these SUMO substrates revealed no substantial difference in expression level of the unmodified form of the substrate protein between HIV-1 infected versus uninfected cells, for all but 6 proteins (Supplemental Figure 2B, red asterisks). This suggests that a large proportion of the substrates we identified show specific increases in SUMO modification upon HIV-1 infection that cannot be explained by increased total protein abundance. All together, our mass spectrometry data indicates that infection with HIV-1 leads to a broad pattern of SUMOylation of HNRNPs and other mediators of alternative splicing.

Experimental validation of HIV-1-induced SUMO targets

To confirm the HIV-1-induced SUMOylations detected by mass spectrometry, we selected 20 putative SUMO1 targets and 14 putative SUMO2 targets for experimental validation in

immunoprecipitation (IP) assays (Figure 2A). In many prior studies, experimental validation of SUMO targets relied on overexpression of tagged SUMOs and/or target proteins. To avoid overexpression artifacts and ensure detection of proteins SUMOylated under physiologically relevant conditions, we immunopreciptated endogenous SUMO-conjugated proteins from HIV-1 infected versus uninfected WT HeLa cells using anti-SUMO1 and anti-SUMO2/3 antibodies. Both SUMO1- and SUMO2/3-conjugates were successfully enriched in the HIV-1-infected and uninfected samples (Figure 2B, C). In the SUMO1 IPs, SUMO1-RanGAP1 is by far the most abundant SUMO-protein conjugate and was used as an additional control given that its level of SUMOylation is unaffected by HIV-1 infection (Figure 2B). Anti-IgG IP was used as a negative control for all IPs.

SUMO1- and SUMO2/3-enriched samples were then analyzed by western blot with antibodies against the endogenous candidate proteins of interest. Using this approach, we were able to detect SUMO-modified forms of 12 SUMO1 targets and 13 SUMO2 targets, as evidenced by the presence of higher molecular weight SUMO-protein conjugates running above the unmodified proteins (Figure 2D, E, arrows) (Supplemental Figure 3). Of these proteins, 4 SUMO1 targets (HNRNPA2B1, HNRNPA3, HNRNPA1, and NACA) and 4 SUMO2/3 targets (HNRNPA2B1, HNRNPA3, HNRNPA0, and HNRNPU) showed a clear increase in one or more SUMO-modified forms following HIV-1 infection, recapitulating our mass spectrometry data (Figure 2D, E). This HIV-1-induced increase in SUMOylation was particularly dramatic for HNRNPs A2B1 and A3 (Figure 2D, E). For both HNRNPs, infection with HIV-1 did not alter the expression level of the unmodified form of the protein (Supplemental Figure 2B, Stars), suggesting a specific increase in SUMOylation. Four of the SUMOylated HNRNPs, including A2B1, A3, A1, and A0, comprise the HNRNPA/B protein family, a structurally and functionally conserved subgroup involved the regulation of transcription, alternative splicing, and translation.[32] Thus, the observed HIV-1-induced SUMOylation of this protein family may represent a novel,

concerted approach used by the HIV-1 virus to manipulate these essential host cell pathways during infection.

A slight increase in SUMOylation following HIV-1 infection was also detected for 9 additional SUMO targets including HNRNPs M, C, and H2, as well as STIP1, DDX47, NOP58, CHORDC1, RPS5, and VIM (Supplemental Figure 3A). However, analysis for these proteins was complicated by low SUMOylation levels and the presence of nonspecific bands detected by the antibodies. Proteins that were SUMOylated basally regardless of HIV-1 infection status are shown in Supplemental Figure 3B. We were unable to detect SUMOylation of 9 proteins, suggesting that these proteins may represent false positives in our mass spectrometry data. Alternatively, given that only a small, 5-10% fraction of many proteins is SUMOylated at any given time,[33] endogenous SUMOylation of these targets may be below our detection level.

Overall, despite the challenges of detecting endogenous SUMOylation, we have demonstrated by both mass spectrometry and biochemical methods that infection with HIV-1 leads to the SUMO-modification of multiple HNRNPs. We selected HNRNPA2B1 (A2/B1) and HNRNPA3 for further study given that both proteins were SUMOylated at a high level, and had a dramatic increase in their modification by both SUMO1 and SUMO2 during HIV-1 infection. For the remainder of this text, we refer to these proteins as A2B1 and A3.

A2B1 and A3 are SUMOylated during HIV-1 infection

In our IP assays, HIV-1 infection led to an increase in four putatively SUMO1- or SUMO2/3-modified forms of A2B1: an abundant SUMO-modified form visible above the unmodified protein even in crude lysates (Figure 2D, E, Supplemental Figure 2B, arrows), and three less abundant, higher molecular weight SUMO-modified forms that were only detectable following enrichment of SUMO (Figure 2D, E, arrows). Here, the abundant form is likely monoSUMOylated A2B1, while the higher molecular weight bands may represent polySUMOylated forms of the protein. Unlike SUMO1, SUMO2/3 contains the SUMOylation consensus sequence and forms chains readily. However, mixed chains with a terminal SUMO1 have been reported.[33,34,35] Therefore the higher

molecular weight forms of A2B1 observed in our assays may represent SUMO1-capped mixed chains. In our IP assays for A3, three SUMO-modified forms of A3 were detected above the unmodified protein even in crude lysates, and were selectively enriched following IP of SUMO1 or SUMO2/3 (Figure 2D, E, arrows). A clear increase in two of these forms was observed following HIV-1-infection, suggesting that although A3 is highly SUMOylated basally, infection with HIV-1 leads to an increase in two specific SUMOylated forms of the protein (Figure 2D, E, arrows).

To confirm that the novel species were indeed due to SUMOylation, we examined the effects of the SUMOylation inhibitor TAK-981[36] on the SUMOylation of A2B1 and A3 during HIV-1 infection. TAK-981 treatment was confirmed to reduce the SUMOylation of RanGAP1 relative to the DMSO control, indicating successful inhibition of SUMOylation (Figure 3A). SUMO1-conjugates were immunoprecipitated from HIV-1-infected cells treated with or without TAK-981, followed by western blot analysis with anti-A2B1 and A3 antibodies. SUMO1 IP samples from uninfected, DMSO-treated cells were used as a control. Here, TAK-981 treatment prevented the HIV-1-induced SUMOylation of both A2B1 and A3, as observed by reduced levels of all SUMOylated forms discussed above relative to the HIV-1-infected, DMSO control (Figure 3B). The level of unmodified A2B1 and A3 was not affected by TAK-981 treatment (Figure 3B). Together, these results suggest that the bands observed in our IP assays represent bonafide SUMO-modified forms of A2B1 and A3. Additionally, IP analysis in the opposite direction (IP of A2B1, followed by western blotting with anti-SUMO1 and anti-SUMO2/3 antibodies) confirmed HIV-1-induced SUMOylation of A2B1 (Supplemental Figure 4A). We have therefore demonstrated by both mass spectrometry and multiple biochemical assays that A2B1 and A3 are SUMOylated during HIV-1 infection.

SUMOylation of A2B1 and A3 requires HIV-1 integration

We next sought to characterize the timing and dependence of A2B1 and A3 SUMOylation on the specific steps of the HIV-1 life cycle. We first infected cells with an HIV-1-GFP reporter virus lacking a functional envelope protein (Figure 3C, “-VSV-G HIV”). Infection with this virus did not

lead to increased A2B1 and A3 SUMOylation, indicating that the SUMO-modification of these proteins is dependent on successful entry of the HIV-1 virion into the host cell (Figure 3C). We next assessed the timing of A2B1 and A3 SUMOylation during HIV-1 infection. SUMO1-conjugates were immunoprecipitated from HIV-1-infected and uninfected controls at 6, 12, 24, and 48 hpi, followed by western blot analysis with anti-A2B1 and A3 antibodies (Figure 3D). At 6 and 12 hpi, there was no difference in the level of SUMOylated A2B1 between the HIV-1-infected samples versus the uninfected controls. However, at both 24 and 48 hpi, increased SUMOylation of A2B1 was readily apparent in the HIV-1 infected samples (Figure 3D). Similarly, the highest level of SUMOylated A3 was detected in the HIV-1 infected samples at 48 hpi, although there was a slight increase in the level of one SUMO1-A3 conjugate as early as 6 hpi (Figure 3D). To explore the range of cells responding to infection with increased SUMOylation, we repeated the experiemnts in additional cell lines. HIV-1 induced SUMOylation of A2B1 and A3 was also observed at 48 hpi in Jurkat cells (an immortalized human T lymphocyte line) and in K562 cells (a chronic myelogenous leukemia cell line), though this phenotype was more dramatic in Jurkat and HeLa cells than in K562 cells (Figure 3E, F).

Integration of the HIV-1 DNA into the host cell genome reportedly occurs at ~15 hpi.[37] Thus, the observed timing of HIV-1-induced SUMOylation of A2B1 and A3 in multiple human cell lines suggests that this modification occurs post-integration, and may depend upon on HIV-1 viral gene products expressed after integration. Additionally, SUMOylation of A2B1 and A3 was <u>not</u> observed upon infection with the retrovirus Moloney Murine Leukemia Virus (MMLV), despite comparable infection efficiencies (Figure 3 G) (Supplemental Figure 4B), suggesting that the SUMOylation of A2B1 and A3 is induced specifically by HIV-1.

Depletion of A2B1 and A3 alters HIV-1 splicing

The activity of A2B1 and A3 is modulated by multiple post-translational modifications such as phosphorylation, ubiquitination, methylation, and SUMOylation[31,32] However, HIV-1-induced SUMOylation of A2B1 and A3, and the functional consequences thereof have not been explored.

Before investigating the function of A2B1 and A3 SUMOylation, we first examined the role of these proteins in the HIV-1 life cycle. Given that A2B1 and A3 regulate host cell alternative splicing,[31,32,38] we focused on the role of A2B1 and A3 in HIV-1 splicing, a process essential for HIV-1 replication.

In HIV-1 infected cells, unspliced (US) viral transcripts encode Gag and Gag-Pro-Pol proteins and serve as the genomic RNA packaged into virions. HIV-1 RNAs can also undergo alternative splicing, where spliced transcripts include a 4-kb class of incompletely spliced (IS) RNAs, and a 2-kb class of completely spliced (CS) RNAs[16,17,18,19] The pattern of HIV-1 splicing has been extensively described and occurs through the use of four splice donor sites (D1-4) and ten splice acceptors (A1-3, A4a, A4b, A4c, A4d, A5, A5b, A7) distributed along the HIV-1 genome. Here, IS RNAs result from splicing between the D1 donor site and one of several splice acceptors: A1 for transcripts encoding the HIV-1 protein Vif, A2 for Vpr, and A4 or A5 for Env/Vpu. CS RNAs result following a second splicing event between D4 and A7, and encode the HIV-1 proteins Tat, Rev, or Nef.[16,17,18,39,40,41] HIV-1 splice site usage is known to be controlled by both *cis*-acting splicing regulatory elements (SREs) and *trans*-acting cellular RBPs, including HNRNPs.[40,42,43] However, the role of A2B1 and A3 in regulating HIV-1 splicing is not well characterized.

To test this role, we utilized a previously described Primer ID-tagged deep sequencing assay[39] to quantify the effects of A2B1 and A3 depletion on the ratio of US, IS, and CS HIV-1 RNAs, and HIV-1 splice acceptor usage. We knocked down A2B1 and A3 in HeLa cells (Figure 4A) followed by infection with VSV-G-pseudotyped HIV-1 (pNL4-3 deltaENV-EGFP). Here, depletion of A2B1 and A3 had no effect on the ratio of US versus total spliced RNAs (Figure 4B). However, within all the spliced classes (comprised of both IS and CS RNAs), loss of A3 led to a dramatic increase in IS RNAs over CS RNAs (Figure 4B'). Additionally, loss of A2B1 led to significantly increased use of the A2 and A3 splice sites (encoding Vpr and Tat transcripts, respectively), and a slight decrease in the use of A1 (encoding Vif transcripts) (Figure 4C). In contrast, loss of HNRNPA3 led to decreased use of the A2 (Vpr) and A4 (Rev/Env) splice sites (Figure 4C) (Supplemental Figure 4A).

Loss of A2B1 inhibits production of infectious HIV-1 virus

Given that the ratio of spliced transcripts and HIV-1 viral proteins produced modulates infectivity,[40] we next tested the role of A2B1 in production of infectious transducing HIV-1 virus. A2B1-KD and control Lenti-X 293T cells (Figure 4D) were transfected with plasmids expressing the HIV-1-GFP reporter virus and the vesicular stomatitis virus (VSV-G) envelope glycoprotein (Figure 4E). Viral supernatants were harvested at 48 hours post-transfection and equal volumes of undilute supernatants were used to infect naïve HeLa cells (Figure 4E). Virus produced from A2B1-KD cells had dramatically reduced infectivity (%GFP+) in comparison to control virus (Figure 4E, F, Supplemental Figure 3B). Cells infected with virus produced from A2B1-KD cells also had an ~3-fold reduction in their level of HIV-1-GFP reporter expression (MFI) relative to control (Figure 4F). Unlike A2B1-KD, A3-KD in the 293T cells led to substantial loss of 293T cell viability. Thus, the effect of A3-KD on virus production was not assessed.

To test whether the reduced infectivity of virus produced by A2B1-KD cells was accompanied by alterations in HIV-1 protein expression, control and A2B1-KD 293T cells and cell culture supernatants were harvested 48 hours post-transfection with the HIV-1-GFP reporter and VSV-G envelope. Virions were pelleted from cell culture supernatants, and the level of Gag in the cells (cell lysate) and released virions (viral pellet) was analyzed by WB (Figure 4G, H). Intriguingly, A2B1-KD had no effect on the level of $pr55^{gag}$ in the virus-producing cells or virions. However, the $pr55^{gag}$ cleavage products $p24^{CA}$ and p17 were reduced in both the A2B1-KD cells and released virions relative to control (Figure 4G, H), suggesting that A2B1-KD may impair Gag processing.

During HIV-1 production, US HIV-1 RNAs are packaged into assembling virions. To test the effect of A2B1 loss on HIV-1 RNA packaging, we extracted RNA from pelleted virions released from control and A2B1-KD 293T cells, and compared the level of GFP RNA by RT-qPCR (Figure 4I). Cellular 7SL RNA is abundantly packaged into HIV-1 virions and was used as an internal control[44] We observed an ~4-fold reduction in the level of HIV-1 RNA in the A2B1-KD virions

relative to the control (Figure 4I), while the level of 7SL RNA in the viral pellet was unaffected by A2B1 KD.

All together, our findings suggest that the effect of A2B1 depletion on HIV-1 virus production is likely multifactorial, and may occur through a combination of effects on transcription, alternative splicing, translation, and/or the packaging of HIV-1 RNAs into virions. This is consistent with the myriad role of A2B1 in regulating multiple aspects of host cell RNA metabolism.[31,32]

DISCUSSION

As intracellular parasites, HIV-1 and other viruses are entirely dependent upon host cellular pathways for completion of their viral life cycles. Viral manipulation of host cell's post-translational modifications, including SUMOylation, thus provides an opportunity to fine tune these host cellular pathways to the viruses' advantage. In this study, we utilized quantitative proteomics to characterize the effect of HIV-1 on the SUMO-modification status of the host cellular proteome. This work represents the first large-scale, unbiased proteomic screen for SUMOylated substrate proteins in the setting of HIV-1 infection. We present evidence that HIV-1 infection leads to a reprogramming of host cell SUMOylation, resulting in the widespread increased SUMO-modification of proteins involved in alternative splicing, or other stages of RNA metabolism (Figure 1E-H). These proteins included numerous heterogeneous nuclear ribonucleoproteins (HNRNPs) and other host cell splicing factors, including the HNRNP A/B protein family (A2B1, A3, A1, and A0), for which HIV-driven SUMOylation was experimentally validated in immunoprecipitation assays (Figure 2D,E). Together, these findings suggest that HIV-driven SUMOylation of HNRNPs may represent an unexplored mechanism by which HIV-1 co-opts host cell RNA metabolism.

We selected HNRNPs A2B1 and A3 for further analysis given that both proteins were shown to be heavily SUMOylated upon HIV-1 infection by both SUMO1 and SUMO2 paralogs, in multiple biochemical assays and in multiple human cell lines (Figure 3 A-G). One intriguing aspect of A2B1 and A3's SUMO-modification is the timing: both proteins were found to be SUMOylated

late in infection (Figure 3D). This timing, combined with the specific induction of A2B1 and A3 SUMOylation by HIV-1 but not the retrovirus MMLV (Figure 3G), suggest that A2B1 and A3 SUMOylation may be triggered by HIV-1 viral gene products expressed after integration of the HIV-1 DNA. Future studies will include testing the dependence of A2B1 and A3 SUMOylation on the presence of functional HIV-1 integrase, and determining the specific HIV-1 viral gene products that are responsible for this modification. The HIV-1 protein Vpr for instance has been shown to modulate multiple host cellular pathways, including alternative splicing of pre-mRNAs.[45,46,47] Thus, the use of HIV-1 genome mutants to test the requirement of Vpr, and other HIV-1 regulatory or accessory proteins for A2B1 and A3 SUMOylation will be valuable.

In addition to the role of HIV-1 gene products in driving this modification, the central question that remains is the functional consequence of HIV-induced A2B1 and A3 SUMOylation. HNRNPs, including A2B1 and A3, are heavily post-translationally modified, where phosphorylation, ubiquitination, methylation, and SUMOylation have been shown to regulate their activity.[31,32] Therefore, there is strong evidence to suspect that HIV-driven SUMOylation modulates the activity of these proteins. To investigate the potential functional consequence of HIV-induced A2B1 and A3 SUMOylation, we focused on the role of these proteins in alternative splicing for two reasons: proper splicing of HIV-1 viral mRNAs is essential for the production of infectious virions, and multiple HNRNPs, including A2B1 and A3, are implicated in the regulation of this process.[40,42,43] In this study, genetic depletion of A2B1 and A3 led to altered HIV-1 splice acceptor site usage (Figure 4C) and/or altered ratios of US, IS, and CS HIV-1 RNAs (Figure 4B, B'). Depletion of A2B1 also dramatically reduced the infectivity of the released virions (Figure 4F, G). Thus, it is possible that aberrant splicing of HIV-1 RNAs resulting from the loss of A2B1 led to the observed reduction in HIV-1 infectivity. However, the picture is potentially more complicated: in addition to splicing, A2B1 and A3 regulate other host cellular RNA pathways exploited by HIV-1, including stabilization, transcription, nuclear export, and translation of mRNAs.[31,32] It is therefore possible that, in addition to an effect on alternative splicing, HIV-induced SUMOylation

of A2B1 and A3 may also modulate A2B1 and A3 activity in other stages of HIV-1 RNA metabolism. In future studies, we will utilize un-SUMOylatable mutants to explore the effect of HIV-driven HNRNP SUMOylation on alternative splicing, and in these additional pathways.

Overall, through a combination of mass spectrometric and biochemical approaches, our study uncovered a novel mechanism potentially underlying the regulation of HIV-1 alternative splicing, a critical step in HIV pathogenesis. Together, our data suggest a concerted mechanism whereby HIV-driven SUMOylation of HNRNPs and other host RNA splicing factors modules the activity of these proteins, in turn modulating the processing of HIV-1 mRNAs.

METHODS AND MATERIALS

Cell culture and cell lines

HeLa and HEK293T cells were maintained in DMEM (Gibco #11965092) supplemented with 10% fetal bovine serum (FBS), 100 units/mL Penicillin-Streptomycin (Gibco #15140122), and 2 mM L-Glutamine (Gibco #25030081). Jurkat cells were maintained in RPMI 1640 medium (Gibco #22400089) supplemented with 10% FBS. All cells were maintained at 37°C in a humidified incubator with 5% CO_2. To generate cell lines stably expressing tagged C-terminal mutant SUMO proteins, 3xFlag-SUMO1^{Q92R}, 3xFlag-SUMO2^{Q88R}, 6His-SUMO1^{Q92R}, and 6His-SUMO2^{Q88R} expression vectors were transfected into HeLa cells using Lipofectamine 3000 (Invitrogen #L3000075). Pooled cells stably expressing the desired proteins were selected using 1 mg/mL Geneticin (Gibco #10131035) and validated by western blot..

Virus production

Lenti-X 293T cells were seeded at a density of $1x10^6$ cells per 10 cm dish one day prior to transfection. Cells were co-transfected with 15 µg of the pNL4-3 deltaENV-EGFP reporter (Centre for AIDS reagents #100616) and 5 µg of the pCMV-VSV-G vector (Addgene #8454) using Lipofectamine 3000 (Invitrogen #L3000075, per manufacturer's protocol) in serum-free DMEM. 6 hours later, transfection media was replaced with serum-containing DMEM. Viral supernatant was

harvested at 48 hours post-transfection, filtered through a 0.45 µm filter, treated with 35 units/mL DNase (Invitrogen #AM2238) at 37°C for 45 min. Viral supernatant was either used directly for infection as described below, or virions in the supernatant were pelleted through a 25% sucrose cushion.

Infection

$3x10^6$ HeLa cells were seeded in 15 cm plates the day prior to infection. Jurkat cells were seeded the day of infection at $5x10^6$ cells per well of a 6 well plate. HeLa and Jurkat cells were incubated with 10 mL or 2 mL viral supernatant, respectively, plus 8 µg/mL Polybrene (Sigma #TR1003G). Virus was removed after 5 hours and replaced with fresh medium. Jurkat cells were resuspended in 10 mL fresh medium, and moved to 10 cm plates until harvest.

Sample preparation for MS

3xFlag-SUMO1^{Q92R}, 3xFlag-SUMO2^{Q87R}, 6His-SUMO1^{Q92R}, and 6His-SUMO2^{Q87R} HeLa cells were seeded and infected with HIV-1 in 15 cm plates as described above. One 15 cm plate was used for each sample and three replicates of each condition were prepared, including uninfected controls. At 24 hpi, cells were harvested using a cell scraper and pelleted by centrifugation (1100 rpm for 5 min.). For 3xFlag-tagged samples, cells were resuspended in 150 µL SDS lysis buffer pre-heated to 95°C (1% SDS, 50 mM Tris/HCl pH 8.0, 150 mM NaCl). Samples were heated at 95°C for 10 min. 500 µL of RIPA w/o SDS (50 mM Tris/HCl pH 8.0, 150 mM NaCl, 1.1% Triton X-100, 0.55% Sodium deoxycholate) was added to each sample, followed by sonication (30-50% power for 3 x 1 sec.) until samples were no longer viscous. 850 µL RIPA w/o SDS was added to each sample, debris was pelleted by centrifugation (13.2K rpm for 10 min. at 4°C), and the supernatant was transferred to fresh tubes. 40 µL of Anti-FLAG M2 Magnetic Beads (Sigma, #M8823) were pre-washed 3x with RIPA (50 mM Tris/HCl pH 8.0, 150 mM NaCl, 1% Triton X-100, 0.5% Sodium deoxycholate, 0.1% SDS) and then added to each sample. Lysates were incubated with beads overnight at 4°C with rotation. The next day, beads were washed 3x with RIPA, and then 3x with RIPA w/o detergent (50 mM Tris/Hcl pH 8.0, 150 mM NaCl). Bound proteins were

eluted in 30 µL elution buffer containing 50 mM Tris/HCL pH 8.0, 150 mM NaCl, 0.05% RapiGest SF Surfactant (Waters) and 100 µg/mL 3xFLAG peptide (MDYKDHDGDYKDHDIDYKDDDDK, Elim Biopharm) for 30 min. at room temperature on a shaker to keep beads suspended. For 6His-tagged samples, samples were prepared as described.[4] Enrichment of Flag and His-tagged proteins were confirmed by western blotting of input, eluates, and flowthrough. The above eluates were used for both total protein analysis and identification of SUMO-conjugated peptides as described below.

LC-MS/MS

An independent mass spectrometry experiment was also performed in collaboration with the lab of Simone Sidoli. of Simone Sidoli. Digested peptides were desalted using a 96-well plate filter (Orochem) packed with 1 mg of Oasis HLB C-18 resin (Waters). Briefly, the samples were resuspended in 100 µl of 0.1% TFA and loaded onto the HLB resin, which was previously equilibrated using 100 µl of the same buffer. After washing with 100 µl of 0.1% TFA, the samples were eluted with a buffer containing 70 µl of 60% acetonitrile and 0.1% TFA and then dried in a vacuum centrifuge. Samples were resuspended in 10 µl of 0.1% TFA and loaded onto a Dionex RSLC Ultimate 300 (Thermo Scientific), coupled online with an Orbitrap Fusion Lumos (Thermo Scientific). Chromatographic separation was performed with a two-column system, consisting of a C-18 trap cartridge (300 µm ID, 5 mm length) and a picofrit analytical column (75 µm ID, 25 cm length) packed in-house with reversed-phase Repro-Sil Pur C18-AQ 3 µm resin. Peptides were separated using a 90 min gradient from 4-30% buffer B (buffer A: 0.1% formic acid, buffer B: 80% acetonitrile + 0.1% formic acid) at a flow rate of 300 nl/min. The mass spectrometer was set to acquire spectra in a data-dependent acquisition (DDA) mode. Briefly, the full MS scan was set to 300-1200 m/z in the orbitrap with a resolution of 120,000 (at 200 m/z) and an AGC target of 5x10e5. MS/MS was performed in the ion trap using the top speed mode (2 secs), an AGC target of 1x10e4 and an HCD collision energy of 35.

Proteome raw files were searched using Proteome Discoverer software (v2.5, Thermo Scientific) using SEQUEST search engine and the SwissProt human + HIV database. Trypsin was specified as the digestive enzyme with up to 2 missed cleavages allowed. Mass tolerance was set to 10 pm for precursor ions and 0.2 Da for product ions. Peptide and protein false discovery rate was set to 1%.

MS data analysis

Protein intensities were $\log_2$ transformed, and $\log_2$ fold changes in SUMO substrates between the HIV-1 infected versus uninfected samples were calculated as the difference between the average $\log_2$ abundance of the triplicate HIV-1-infected samples and uninfected samples (Supplemental Table 1 tabs C-F, Supplemental Table 2).

Endogenous SUMO immunoprecipitation

Immunoprecipitation of SUMO1 or SUMO2/3 conjugated proteins was performed as described[33] for non-denatured lysates using 50 µL of SUMO1 (Santa Cruz # sc-5308-AC), or SUMO2/3/4 (Santa Cruz # sc-393144 AC) antibody beads per sample in the presence of 15 mM NEM (Sigma #E3876). (SUMO4 is expressed in HeLa at very low levels relative to SUMO1 and SUMO2/3. Thus, the above antibody was used to immunoprecipitated predominantly SUMO2/3-conjugates in this cell line). Mouse IgG-Agarose (Sigma # A0919) was used a control. Immunoprecipitated proteins were eluted in 30 µL Laemmli buffer for 5 min. at 95°C on a shaker. Eluates were loaded directly on a gel for western blotting as described below.

Western blotting

Lysates were prepared using a Millipore Whole Cell Extraction Kit (#2910). Protein content was quantified by Pierce BCA Protein Assay (Thermofisher #23227). Samples were separated on 4-20% Mini-PROTEAN TGX Precast Gels (Bio-Rad #4561096) after heat denaturation in Laemmli buffer. Proteins were transferred to nitrocellulose membranes (Bio-Rad #1620115) using a Transblot-Turbo Transfer System (BioRad). Membranes were blocked in 5% nonfat milk in TBS-T, probed with primary antibodies overnight (4°C), and incubated with HRP-conjugated secondary

antibodies for 1.5h at room temperature. Proteins were detected using SuperSignal West Femto Maximum Sensitivity Substrate (Thermofisher #36095) on an iBright 1500 Imaging System (Thermofisher). Protein levels were quantified using Image Lab (Bio-Rad).

Antibodies

Primary antibodies	Catalog #	Dilution
Monoclonal ANTI-FLAG M2 (Mouse)	Sigma, F3165	1:1000
Monoclonal anti-polyHistidine Antibody (Mouse)	Sigma, H1029	1:1000
Human SUMO Pan Specific Antibody (Rat)	RD Systems, A-714	1:1000
SUMO1 Monoclonal Antibody (21C7) (Mouse)	Invitrogen, 332400	1:1000
mAb to Sumo2 + Sumo3 [8A2] (Mouse)	Abcam, AB81371	1:1000
Anti-GAPDH mAb (6C5) (Mouse)	Millipore, CB1001	1:1000
RanGAP1 (D2T7T) Rabbit mAb	Cell Signaling, 36067S	1:1000
HNRNPA2B1 pAb (Rabbit)	Proteintech, 14813-1-AP	1:1000
HNRNPA3 PolyAb (Rabbit)	Proteintech, 25142-1-AP	1:1000
NACA Polyclonal Antibody (Rabbit)	Invitrogen, 401000	3 µg/mL
HADHB PolyAb (Rabbit)	Proteintech, 29091-1-AP	1:1000
mAb to HNRPH2/HNRNPH2 [EPR12171] (Rabbit)	Abcam, AB181171	1:1000
HNRNPR PolyAb (Rabbit)	Proteintech, 29980-1-AP	1:1000
CCAR1 PolyAb (Rabbit)	Proteintech, 25232-1-AP	1:1000
RPS5 PolyAb (Rabbit)	Proteintech, 16964-1-AP	1:1000
Vimentin PolyAb (Rabbit)	Proteintech, 10366-1-AP	1:1000
HERC5 PolyAb (Rabbit)	Proteintech, 22692-1-AP	1:1000
CHORDC1 PolyAb (Rabbit)	Proteintech, 25525-1-AP	1:1000
RUVBL2 PolyAb (Rabbit)	Proteintech, 10195-1-AP	1:1000
UGDH PolyAb (Rabbit)	Proteintech, 13151-1-AP	1:1000

NOP58 PolyAb (Rabbit)	Proteintech, 14409-1-AP	1:1000
Histone H1.4 Rabbit mAb (D4J5Q)	Cell Signaling, 41328S	1:1000
DDX47 PolyAb (Rabbit)	Proteintech, 17795-1-AP	1:1000
UQCRFS1 PolyAb (Rabbit)	Proteintech, 18443-1-AP	1:1000
ACTL6A PolyAb (Rabbit)	Proteintech, 10341-1-AP	1:1000
KHSRP PolyAb (Rabbit)	Proteintech, 55409-1-AP	1:1000
HNRNPM PolyAb (Rabbit)	Proteintech, 26897-1-AP	1:1000
HNRNPA1 PolyAb (Rabbit)	Proteintech, 11176-1-AP	1:1000
SRRM2 mAb (Rabbit)	Abcam, AB317817	1:1000
PHF5A PolyAb (Rabbit)	Proteintech, 15554-1-AP	1:1000
STIP1 PolyAb (Rabbit)	Proteintech, 15218-1-AP	1:1000
HNRNPA0 PolyAb (Rabbit)	Proteintech, 10848-1-AP	1:1000
TAF15 PolyAb (Rabbit)	Proteintech, 25521-1-AP	1:1000
TRA2B PolyAb (Rabbit)	Proteintech, 29627-1-AP	1:1000
HNRNPU PolyAb (Rabbit)	Proteintech, 16365-1-AP	1:1000
HNRNPC PolyAb (Rabbit)	Proteintech, 11760-1-AP	1:1000
SRSF6 PolyAb (Rabbit)	Proteintech, 11772-1-AP	1:1000
pAb to HIV1 p55 + p24 + p17 (Rabbit)	Abcam, AB63917	1:2000
Vpr PolyAb (Rabbit)	Proteintech, 51143-1-AP	1:1000
mAb to HIV1 Nef (Mouse)	Abcam, AB42355	1:1000
Anti-HIV1 Vif antibody (Mouse)	Abcam, ab66643	1:1000
Anti-HIV1 Rev antibody (Mouse)	Abcam, ab85529	1:1000
Anti-HIV1 Tat antibody (Rabbit)	Abcam, ab43014	1:1000
Anti-GFP antibody (Rabbit)	Abcam, ab290	1:1000

hnRNPA2/B1 (B-7) (AC) (used for HNRNPA2B1 IPs)	Santa Cruz, sc-374053 AC	50 µL per IP
Rabbit anti-HNRNPA3 (used for HNRNPA3 IPs)	Bethyl, A305-815A-T	3 µg per IP
Normal Rabbit IgG (used as Control for HNRNPA3 IPs)	Cell Signaling, 2729S	3 µg per IP

Secondary antibodies	Catalog #	Dilution
ECL Anti-Mouse IgG HRP-linked whole antibody	Amersham, NXA931V	1:10,000
ECL Anti-Rabbit IgG HRP-linked whole antibody	Amersham, NA934V	1:10,000
EasyBlot anti Rat IgG (HRP)	GeneTex, GTX628474-01	1:10,000

siRNA knockdowns

Cells were plated at $1x10^5$ cells/well of a 6-well plate one day prior to transfection. ON-TARGETplus Human HNRNPA2B1, HNRNPA3, and Non-targeting SMARTpool siRNAs (Dharmacon #s L-011690-01-0005, L-019347-00-0005, and D-001810-10-05) were diluted to stock concentrations of 20 µM. Cells were transfected by dropwise addition of a mixture containing 5 µL of the 20 µM siRNA stocks, 5 µL Lipofectamine RNAiMAX (Invitrogen #13778500) and 490 µL Opti-MEM (Gibco #51985034) at 24 hours post-plating, and again at 48 hours post-plating.

RNA extraction

Total RNA was extracted using Quick-RNA Miniprep Plus Kit (Zymo #R1058).

Bioinformatic analysis

GO enrichment analysis was performed with g:Profiler using the Reactome database and Benjamini-Hochberg method to calculate FDR values, where a 5% FDR cutoff was used to select significantly enriched pathways.

Flow cytometry

Percentages of GFP+ cells and mean fluorescence intensity (MFI) was measured using a BD LSRII or LSRFortessa (BD Biosciences). Viable cells were gated using FSC-A and SSC-A plots, and FITC-A and FSC-A plots were used to gate the GFP+ population. MFI was determined after gating the GFP+ population.

qPCR

RNA was extracted as described above. cDNA was synthesized using SuperScript III First-Strand Synthesis SuperMix (Invitrogen #11752-050). qPCR was performed on a 7500 Fast Real-Time PCR System using FastStart Universal SYBR Green Master (ROX) (Roche #4913850001). All reactions were performed in triplicate using the following primers: EGFP (forward 5' AAGGGCGAGGAGCTGTTCACC 3', reverse 5' GTGGTCACGAGGGTGGGCCAG 3'), 7SL (forward 5'ATCGGGTGTCCGCACTAAG 3', reverse 5' CACCCCTCCTTAGGCAACCT).

Compounds

10 mM Subasumstat (TAK-981) in 1 mL DMSO was purchased from MedChemExpress (#HY-111789).

Cell viability assay

Cell viability was assessed using Cell Proliferation Reagent WST-1 (Roche #5015944001) per manufacturer's instructions.

Statistics

Statistical analysis was performed using GraphPad Prism 10 or Microsoft Excel. Error bars indicate mean ± SEM of at least three independent experiments. Significance was determined by unpaired two-tailed t test unless otherwise specified, where $p<0.05$ was considered statistically significant.

Data and Software Availability

All additional data is available upon request. Software used is commercially available. Illustrations were created using BioRender.com.

ACKNOWLEDGMENTS

This study was funded by Center for Structural Biology of HIV RNA (CRNA) Grant# U54 AI170660, Herbert Irving Comprehensive Cancer Center (HICCC) Grant #P30CA013696, and NIH 1 R01 AI178848.

REFERENCES

1. Liang, T., Li, G., Lu, Y., Hu, M., and Ma, X. (2023). The Involvement of Ubiquitination and SUMOylation in Retroviruses Infection and Latency. Viruses 15. 10.3390/v15040985.
2. Imbert, F., and Langford, D. (2021). Viruses, SUMO, and immunity: the interplay between viruses and the host SUMOylation system. J Neurovirol 27, 531-541. 10.1007/s13365-021-00995-9.
3. Lork, M., Lieber, G., and Hale, B.G. (2021). Proteomic Approaches to Dissect Host SUMOylation during Innate Antiviral Immune Responses. Viruses 13. 10.3390/v13030528.
4. Tammsalu, T., Matic, I., Jaffray, E.G., Ibrahim, A.F.M., Tatham, M.H., and Hay, R.T. (2014). Proteome-wide identification of SUMO2 modification sites. Sci Signal 7, rs2. 10.1126/scisignal.2005146.
5. Hendriks, I.A., D'Souza, R.C., Yang, B., Verlaan-de Vries, M., Mann, M., and Vertegaal, A.C. (2014). Uncovering global SUMOylation signaling networks in a site-specific manner. Nat Struct Mol Biol 21, 927-936. 10.1038/nsmb.2890.
6. Domingues, P., Golebiowski, F., Tatham, M.H., Lopes, A.M., Taggart, A., Hay, R.T., and Hale, B.G. (2015). Global Reprogramming of Host SUMOylation during Influenza Virus Infection. Cell Rep 13, 1467-1480. 10.1016/j.celrep.2015.10.001.
7. Barroso-Gomila, O., Trulsson, F., Muratore, V., Canosa, I., Merino-Cacho, L., Cortazar, A.R., Perez, C., Azkargorta, M., Iloro, I., Carracedo, A., et al. (2021). Identification of proximal SUMO-dependent interactors using SUMO-ID. Nat Commun 12, 6671. 10.1038/s41467-021-26807-6.
8. Fan, Y., Li, X., Zhang, L., Zong, Z., Wang, F., Huang, J., Zeng, L., Zhang, C., Yan, H., Zhang, L., and Zhou, F. (2022). SUMOylation in Viral Replication and Antiviral Defense. Adv Sci (Weinh) 9, e2104126. 10.1002/advs.202104126.
9. Colomer-Lluch, M., Castro-Gonzalez, S., and Serra-Moreno, R. (2020). Ubiquitination and SUMOylation in HIV Infection: Friends and Foes. Curr Issues Mol Biol 35, 159-194. 10.21775/cimb.035.159.
10. Mete, B., Pekbilir, E., Bilge, B.N., Georgiadou, P., Celik, E., Sutlu, T., Tabak, F., and Sahin, U. (2022). Human immunodeficiency virus type 1 impairs sumoylation. Life Sci Alliance 5. 10.26508/lsa.202101103.
11. Gurer, C., Berthoux, L., and Luban, J. (2005). Covalent modification of human immunodeficiency virus type 1 p6 by SUMO-1. J Virol 79, 910-917. 10.1128/JVI.79.2.910-917.2005.
12. Zamborlini, A., Coiffic, A., Beauclair, G., Delelis, O., Paris, J., Koh, Y., Magne, F., Giron, M.L., Tobaly-Tapiero, J., Deprez, E., et al. (2011). Impairment of human immunodeficiency virus type-1 integrase SUMOylation correlates with an early replication defect. J Biol Chem 286, 21013-21022. 10.1074/jbc.M110.189274.

13. Li, Z., Wu, S., Wang, J., Li, W., Lin, Y., Ji, C., Xue, J., and Chen, J. (2012). Evaluation of the interactions of HIV-1 integrase with small ubiquitin-like modifiers and their conjugation enzyme Ubc9. Int J Mol Med 30, 1053-1060. 10.3892/ijmm.2012.1088.
14. Madu, I.G., Li, S., Li, B., Li, H., Chang, T., Li, Y.J., Vega, R., Rossi, J., Yee, J.K., Zaia, J., and Chen, Y. (2015). A Novel Class of HIV-1 Antiviral Agents Targeting HIV via a SUMOylation-Dependent Mechanism. Sci Rep 5, 17808. 10.1038/srep17808.
15. Irwan, I.D., Bogerd, H.P., and Cullen, B.R. (2022). Epigenetic silencing by the SMC5/6 complex mediates HIV-1 latency. Nat Microbiol 7, 2101-2113. 10.1038/s41564-022-01264-z.
16. Purcell, D.F., and Martin, M.A. (1993). Alternative splicing of human immunodeficiency virus type 1 mRNA modulates viral protein expression, replication, and infectivity. J Virol 67, 6365-6378. 10.1128/JVI.67.11.6365-6378.1993.
17. Stoltzfus, C.M. (2009). Chapter 1. Regulation of HIV-1 alternative RNA splicing and its role in virus replication. Adv Virus Res 74, 1-40. 10.1016/S0065-3527(09)74001-1.
18. Karn, J., and Stoltzfus, C.M. (2012). Transcriptional and posttranscriptional regulation of HIV-1 gene expression. Cold Spring Harb Perspect Med 2, a006916. 10.1101/cshperspect.a006916.
19. Emery, A., and Swanstrom, R. (2021). HIV-1: To Splice or Not to Splice, That Is the Question. Viruses 13. 10.3390/v13020181.
20. Pozzi, B., Mammi, P., Bragado, L., Giono, L.E., and Srebrow, A. (2018). When SUMO met splicing. RNA Biol 15, 689-695. 10.1080/15476286.2018.1457936.
21. Acuna, M.L., Garcia-Morin, A., Orozco-Sepulveda, R., Ontiveros, C., Flores, A., Diaz, A.V., Gutierrez-Zubiate, I., Patil, A.R., Alvarado, L.A., Roy, S., et al. (2023). Alternative splicing of the SUMO1/2/3 transcripts affects cellular SUMOylation and produces functionally distinct SUMO protein isoforms. Sci Rep 13, 2309. 10.1038/s41598-023-29357-7.
22. Desterro, J.M., Rodriguez, M.S., and Hay, R.T. (1998). SUMO-1 modification of IkappaBalpha inhibits NF-kappaB activation. Mol Cell 2, 233-239. 10.1016/s1097-2765(00)80133-1.
23. Colomer-Lluch, M., and Serra-Moreno, R. (2017). BCA2/Rabring7 Interferes with HIV-1 Proviral Transcription by Enhancing the SUMOylation of IkappaBalpha. J Virol 91. 10.1128/JVI.02098-16.
24. Bueno, M.T., Garcia-Rivera, J.A., Kugelman, J.R., Morales, E., Rosas-Acosta, G., and Llano, M. (2010). SUMOylation of the lens epithelium-derived growth factor/p75 attenuates its transcriptional activity on the heat shock protein 27 promoter. J Mol Biol 399, 221-239. 10.1016/j.jmb.2010.03.063.
25. Martinat, C., Cormier, A., Tobaly-Tapiero, J., Palmic, N., Casartelli, N., Mahboubi, B., Coggins, S.A., Buchrieser, J., Persaud, M., Diaz-Griffero, F., et al. (2021). SUMOylation of SAMHD1 at Lysine 595 is required for HIV-1 restriction in non-cycling cells. Nat Commun 12, 4582. 10.1038/s41467-021-24802-5.
26. Galisson, F., Mahrouche, L., Courcelles, M., Bonneil, E., Meloche, S., Chelbi-Alix, M.K., and Thibault, P. (2011). A novel proteomics approach to identify SUMOylated proteins and their modification sites in human cells. Mol Cell Proteomics 10, M110 004796. 10.1074/mcp.M110.004796.
27. Matunis, M.J., Coutavas, E., and Blobel, G. (1996). A novel ubiquitin-like modification modulates the partitioning of the Ran-GTPase-activating protein RanGAP1 between the cytosol and the nuclear pore complex. J Cell Biol 135, 1457-1470. 10.1083/jcb.135.6.1457.
28. Hendriks, I.A., and Vertegaal, A.C. (2016). A comprehensive compilation of SUMO proteomics. Nat Rev Mol Cell Biol 17, 581-595. 10.1038/nrm.2016.81.
29. Zhou, D., Hayashi, T., Jean, M., Kong, W., Fiches, G., Biswas, A., Liu, S., Yosief, H.O., Zhang, X., Bradner, J., et al. (2020). Inhibition of Polo-like kinase 1 (PLK1) facilitates the

elimination of HIV-1 viral reservoirs in CD4(+) T cells ex vivo. Sci Adv 6, eaba1941. 10.1126/sciadv.aba1941.
30. Ma, X., Yang, T., Luo, Y., Wu, L., Jiang, Y., Song, Z., Pan, T., Liu, B., Liu, G., Liu, J., et al. (2019). TRIM28 promotes HIV-1 latency by SUMOylating CDK9 and inhibiting P-TEFb. Elife 8. 10.7554/eLife.42426.
31. Geuens, T., Bouhy, D., and Timmerman, V. (2016). The hnRNP family: insights into their role in health and disease. Hum Genet 135, 851-867. 10.1007/s00439-016-1683-5.
32. Liu, Y., and Shi, S.L. (2021). The roles of hnRNP A2/B1 in RNA biology and disease. Wiley Interdiscip Rev RNA 12, e1612. 10.1002/wrna.1612.
33. Xiao, Y., Pollack, D., Nieves, E., Winchell, A., Callaway, M., and Vigodner, M. (2015). Can your protein be sumoylated? A quick summary and important tips to study SUMO-modified proteins. Anal Biochem 477, 95-97. 10.1016/j.ab.2014.11.006.
34. Rodriguez, M.S., Dargemont, C., and Hay, R.T. (2001). SUMO-1 conjugation in vivo requires both a consensus modification motif and nuclear targeting. J Biol Chem 276, 12654-12659. 10.1074/jbc.M009476200.
35. De La Cruz-Herrera, C.F., Tatham, M.H., Siddiqi, U.Z., Shire, K., Marcon, E., Greenblatt, J.F., Hay, R.T., and Frappier, L. (2023). Changes in SUMO-modified proteins in Epstein-Barr virus infection identifies reciprocal regulation of TRIM24/28/33 complexes and the lytic switch BZLF1. PLoS Pathog 19, e1011477. 10.1371/journal.ppat.1011477.
36. Langston, S.P., Grossman, S., England, D., Afroze, R., Bence, N., Bowman, D., Bump, N., Chau, R., Chuang, B.C., Claiborne, C., et al. (2021). Discovery of TAK-981, a First-in-Class Inhibitor of SUMO-Activating Enzyme for the Treatment of Cancer. J Med Chem 64, 2501-2520. 10.1021/acs.jmedchem.0c01491.
37. Murray, J.M., Kelleher, A.D., and Cooper, D.A. (2011). Timing of the components of the HIV life cycle in productively infected CD4+ T cells in a population of HIV-infected individuals. J Virol 85, 10798-10805. 10.1128/JVI.05095-11.
38. Komuro, R., Honda, Y., Yanaizu, M., Nagahama, M., and Kino, Y. (2023). Alzheimer's Disease-Associated Alternative Splicing of CD33 Is Regulated by the HNRNPA Family Proteins. Cells 12. 10.3390/cells12040602.
39. Emery, A., Zhou, S., Pollom, E., and Swanstrom, R. (2017). Characterizing HIV-1 Splicing by Using Next-Generation Sequencing. J Virol 91. 10.1128/JVI.02515-16.
40. Sertznig, H., Hillebrand, F., Erkelenz, S., Schaal, H., and Widera, M. (2018). Behind the scenes of HIV-1 replication: Alternative splicing as the dependency factor on the quiet. Virology 516, 176-188. 10.1016/j.virol.2018.01.011.
41. Nguyen Quang, N., Goudey, S., Segeral, E., Mohammad, A., Lemoine, S., Blugeon, C., Versapuech, M., Paillart, J.C., Berlioz-Torrent, C., Emiliani, S., and Gallois-Montbrun, S. (2020). Dynamic nanopore long-read sequencing analysis of HIV-1 splicing events during the early steps of infection. Retrovirology 17, 25. 10.1186/s12977-020-00533-1.
42. Fu, X.D., and Ares, M., Jr. (2014). Context-dependent control of alternative splicing by RNA-binding proteins. Nat Rev Genet 15, 689-701. 10.1038/nrg3778.
43. Kutluay, S.B., Emery, A., Penumutchu, S.R., Townsend, D., Tenneti, K., Madison, M.K., Stukenbroeker, A.M., Powell, C., Jannain, D., Tolbert, B.S., et al. (2019). Genome-Wide Analysis of Heterogeneous Nuclear Ribonucleoprotein (hnRNP) Binding to HIV-1 RNA Reveals a Key Role for hnRNP H1 in Alternative Viral mRNA Splicing. J Virol 93. 10.1128/JVI.01048-19.
44. Onafuwa-Nuga, A.A., Telesnitsky, A., and King, S.R. (2006). 7SL RNA, but not the 54-kd signal recognition particle protein, is an abundant component of both infectious HIV-1 and minimal virus-like particles. RNA 12, 542-546. 10.1261/rna.2306306.
45. Li, G., Bukrinsky, M., and Zhao, R.Y. (2009). HIV-1 viral protein R (Vpr) and its interactions with host cell. Curr HIV Res 7, 178-183. 10.2174/157016209787581436.

46. Kuramitsu, M., Hashizume, C., Yamamoto, N., Azuma, A., Kamata, M., Yamamoto, N., Tanaka, Y., and Aida, Y. (2005). A novel role for Vpr of human immunodeficiency virus type 1 as a regulator of the splicing of cellular pre-mRNA. Microbes Infect 7, 1150-1160. 10.1016/j.micinf.2005.03.022.
47. Hashizume, C., Kuramitsu, M., Zhang, X., Kurosawa, T., Kamata, M., and Aida, Y. (2007). Human immunodeficiency virus type 1 Vpr interacts with spliceosomal protein SAP145 to mediate cellular pre-mRNA splicing inhibition. Microbes Infect 9, 490-497. 10.1016/j.micinf.2007.01.013.

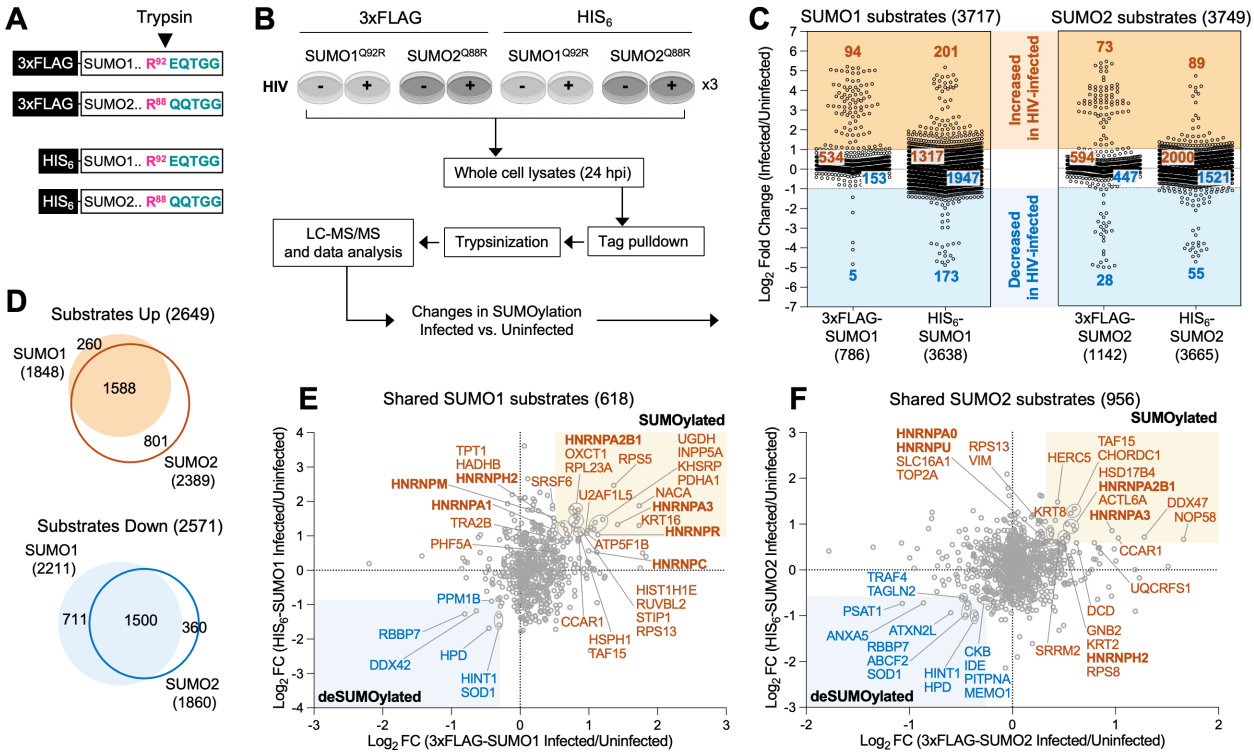

Biological pathway	Gene name
Metabolism of RNA	CCAR1, HNRNPA1/A2B1/A3/C/H2/M/R, KHSRP, PHF5A, PSMD4, SET
mRNA splicing	SRSF6, TRA2B, HNRNPA1/A2B1/A3/C/H2/M/R, PHF5A, CCAR1
Processing of pre-mRNA	SRSF6, TRA2B, HNRNPA1/A2B1/A3/C/H2/M/R, PHF5A, CCAR1

Biological pathway	Gene name
Metabolism of RNA	DDX47, HNRNPA2B1/A3/H2,CCAR1, NOP58, RPS8, SRRM2, EMG1, RPL13A, RPL6
rRNA processing	DDX47, NOP58, RPS8, EMG1, RPL13A/L6
mRNA splicing	HNRNPA2B1/A3/H2, CCAR1, SRRM2
Processing of pre-mRNA	HNRNPA2B1/A3/H2, CCAR1, SRRM2

Figure 1. Proteome-wide identification of proteins SUMOylated during HIV-1 infection. (A) 3xFLAG and HIS_6-tagged mutant SUMO expression vectors. Tryptic digest leaves an -EQTGG or -QQTGG signature remnant on SUMO1 or SUMO2 modified peptides, respectively. **(B)** Overview of proteomic strategy to identify proteins with a change in SUMOylation status during HIV-1 infection. Three replicates were performed per condition. **(C)** Log_2 fold changes in SUMO1 and SUMO2 substrate abundance (y-axis, Infected/Uninfected) in the 3xFLAG or HIS_6-tagged SUMO cell lines following HIV-1 infection (x-axis). Orange and blue shaded areas

designate substrates with a Log_2 fold change >1 or < -1 (>2-fold linear change up or down, respectively). The numbers of substrates identified in each cell line and each category are indicated. **(D)** Overlap between SUMO1 and SUMO2 substrates that were increased or decreased by HIV-1 infection. **(E, F)** Graphs indicating changes in abundance to SUMO1 (E) and SUMO2 (F) substrates derived from 3xFLAG-tagged SUMO cells (x-axis) versus the respective HIS_6-tagged SUMO cells (y-axis) in response to HIV-1 infection. Log_2FC = Log_2 fold change. Substrates with fold changes in the top or bottom quartiles in both the 3xFLAG- and HIS_6-tagged SUMO samples are highlighted, in addition select splicing factors indicated in G, H. **(G, H)** Significantly enriched pathways in the HIV-induced SUMO1 and SUMO2 substrates common to the 3xFLAG- and HIS_6-tagged SUMO samples shown in parts E and F. Select genes included in these pathways are shown in the tables below.

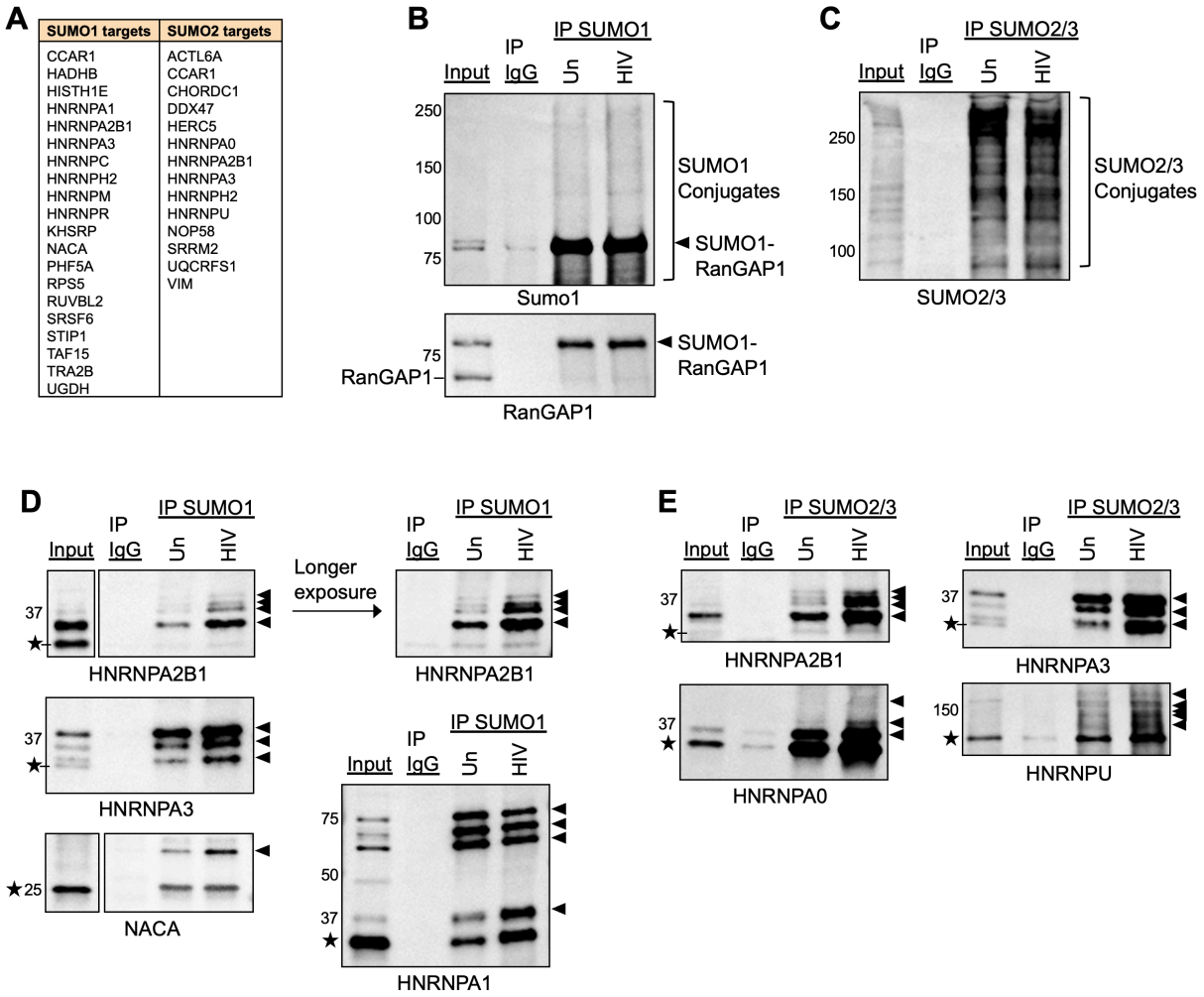

Figure 2. Experimental validation of HIV-1 induced SUMO targets. (A) List of putative HIV-1-induced SUMO1 and SUMO2 targets tested experimentally. **(B,C)** Western blots showing enrichment of SUMO1-conjugates, SUMO1-modified RanGAP1, and SUMO2/3-conjugates following immunoprecipitation with the indicated anti-SUMO antibodies in HIV-1-infected ("HIV") versus uninfected controls ("Un") at 24 hpi. **(D, E)** Western blot analysis of SUMO1- or SUMO2/3-enriched samples from HIV-1-infected cells ("HIV") versus uninfected controls ("Un"). SUMO-conjugates were immunoprecipitated using anti-SUMO1 or SUMO2/3 antibodies at 24 hpi, and samples were analyzed by western blot for the indicated substrates. Stars indicate unmodified proteins. Arrowheads indicate SUMO-conjugated proteins. Crude lysate from HIV-1-

infected cells was used as input for IPs, where input was 5% protein loaded in IPs. Non-immune IgG = IP control.

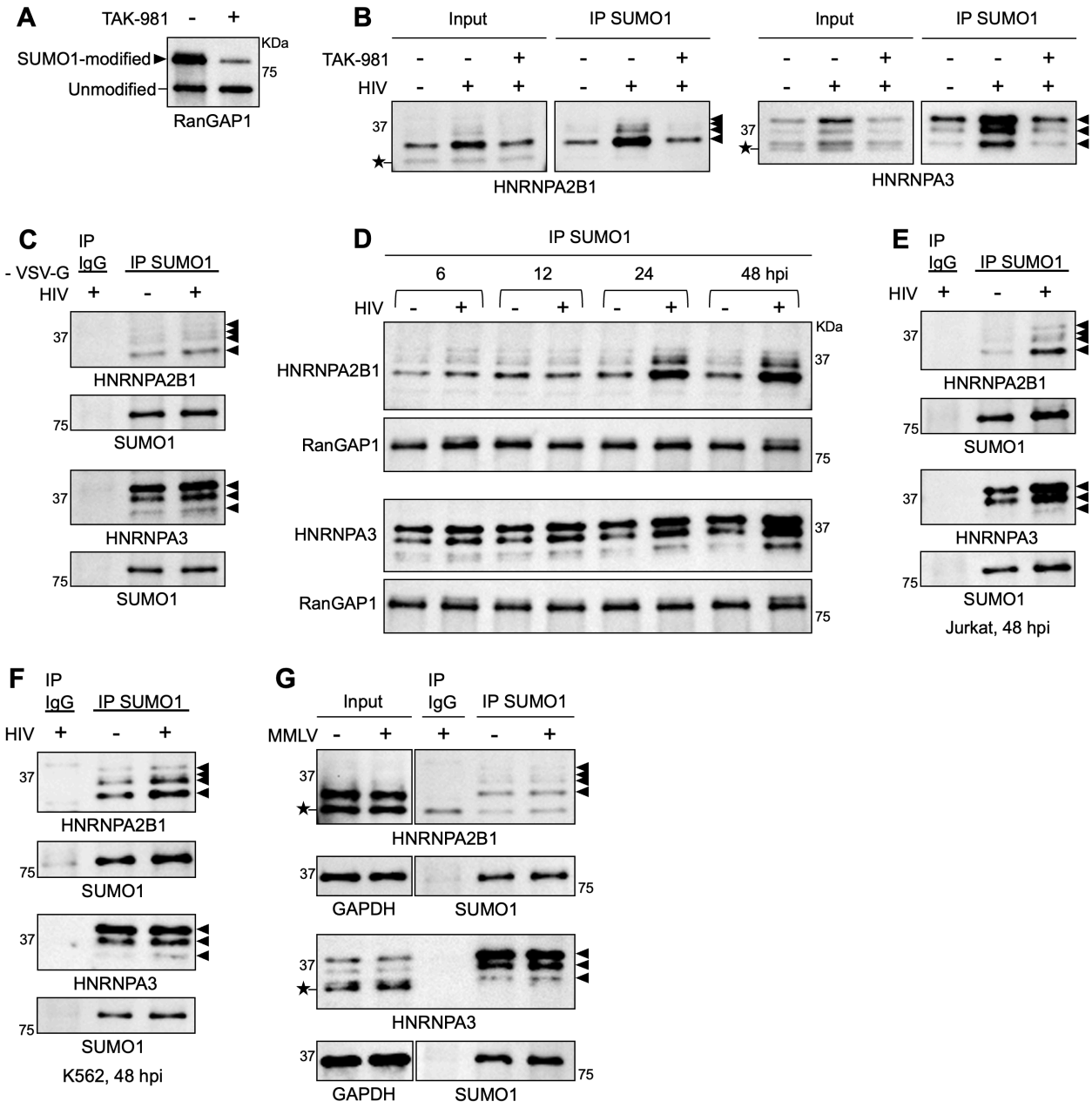

Figure 3. HNRNPs A2B1 and A3 are SUMOylated during HIV-1 infection. (A) Western blot showing the level of SUMO1-modified and unmodified RanGAP1 in HeLa cells treated with the SUMOylation inhibitor TAK-981 versus the DMSO control ("-"). **(B)** Western blot showing the level of SUMO1-conjugated A2B1 and A3 in HIV-1-infected cells treated with or without TAK-981. Uninfected, untreated cells were used as a control. Crude lysate from the corresponding conditions was used as input for IPs (5% of total protein loaded in IPs). For both A and B, TAK-

981 was used at a concentration of 12 μM. DMSO = untreated control. **(C)** Western blot analysis of SUMO1-modified A2B1 and A3 in cells infected with Env mutant HIV-1 (pNL4-3 deltaENV-EGFP) lacking the VSV-G envelope ("-VSV-G HIV") versus the uninfected control. Cells were harvested at 48 hpi. **(D)** Western blot showing the level of SUMO-modified A2B1 or A3 in HIV-1-infected HeLa cells versus uninfected controls at 6, 12, 24, and 48 hpi. **(E, F)** Western blot analysis of SUMO1-modified A2B1 and A3 in HIV-1-infected Jurkat cells (E) or K562 cells (F) versus uninfected controls at 48 hpi. **(G)** Western blot analysis of SUMO1-modified A2B1 and A3 in MMLV-infected HeLa cells versus uninfected controls. Cells were infected with VSV-G pseudotyped MMLV (pNCA-GFP) and harvested at 48 hpi for lysate preparation. Crude lysate input for each condition is shown for comparison. For all, SUMO1-conjugated proteins were immunoprecipitated using anti-SUMO1 antibodies and samples were analyzed by western blot for A2B1 and A3. Arrows indicate SUMO1-modified proteins. Stars indicate unmodified proteins. For C-G, non-immune IgG = IP control and SUMO1-modified RanGAP1 = loading control for IPs.

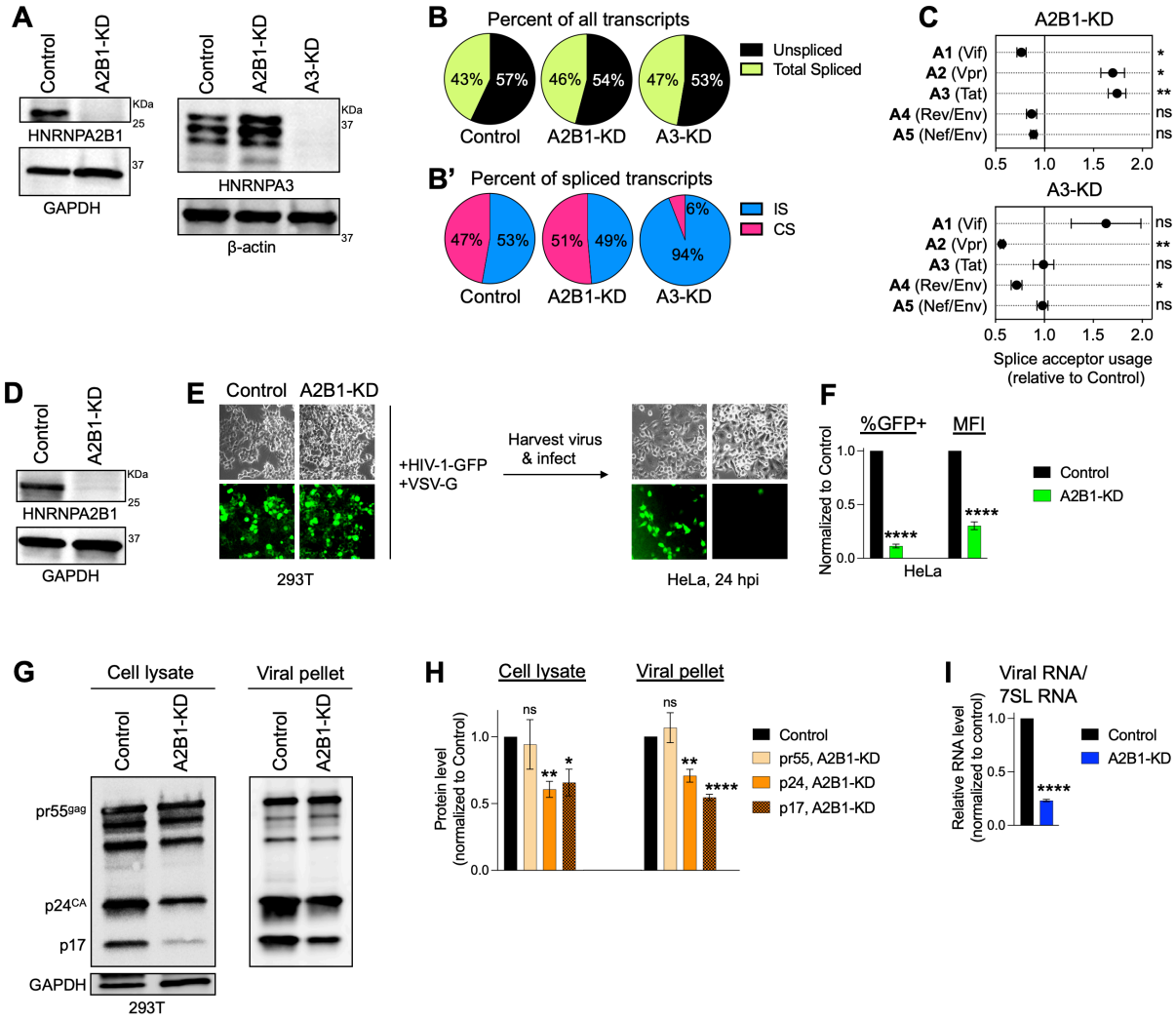

Figure 4. Depletion of HNRNPs A2B1 and A3 alters HIV-1 splicing and infectivity. (A) Western blot showing A2B1 and A3 expression in HeLa cells transfected with Control, A2B1, or A3 siRNAs. **(B)** Quantification of Unspliced and total Spliced HIV-1 RNAs in siRNA Control versus A2B1- or A3-knockdown (KD) cells. Circle proportions represent percent of all transcripts. Cells were infected with VSV-G pseudotyped HIV-1-GFP reporter virus and HIV-1 splicing was quantified at 24 hpi. **(B')** Quantification of incompletely spliced (IS) and completely spliced (CS) HIV-1 RNAs in Control vs. A2B1-KD and A3-KD samples at 24 hpi. Circle proportions represent percent of spliced transcripts. **(C)** Analysis of final splicing events occurring at HIV-1 splice acceptors A1 through A5 in A2B1-KD and A3-KD samples. HIV-1

proteins resulting from use of each splice acceptor is listed in parenthesis. Splice acceptor usage is represented as fold change relative to the siRNA Control. **(D)** Western blot showing A2B1 expression in Lenti-X 293T cells transfected with Control versus A2B1 siRNAs. **(E)** Control and A2B1-KD cells from (D) were co-transfected with plasmids expressing the HIV-1-GFP reporter genome and the VSV-G envelope. Cell culture supernatants were collected at 48 hours post-transfection and used to infect HeLa cells. **(F)** Flow cytometric measurement of the percentage of GFP+ cells and GFP MFI in HIV-1-infected HeLa cells from (F) at 24 hpi. **(G)** Western blot showing expression of HIV-1 Gag cleavage products in Control versus A2B1-KD 293T cells (Cell Lysate) and in released virions (Viral Pellet) after transfection with plasmids expressing the HIV-1 viral genome and VSV-G envelope. Cells were harvested for lysate preparation at 48 hpi and virions in the supernatants were isolated by pelleting through a 25% sucrose cushion. **(H)** Densitometric analysis of data from (H) shown relative to Control. **(I)** RT-qPCR analysis of HIV-1 viral RNA in the virions released from Control versus A2B1-KD cells. 7SL RNA was used as an internal control. (error bars = mean ± SEM of three independent experiments unless otherwise stated; for splicing analysis, siRNA Control and A2B1-KD sample data was derived from two independent experiments each with three technical replicates, data for A3-KD samples includes two technical replicates from one experiment; unpaired t-test,****$p \leq 0.0001$,***$p \leq 0.001$,**$p \leq 0.01$,*$p \leq 0.05$).

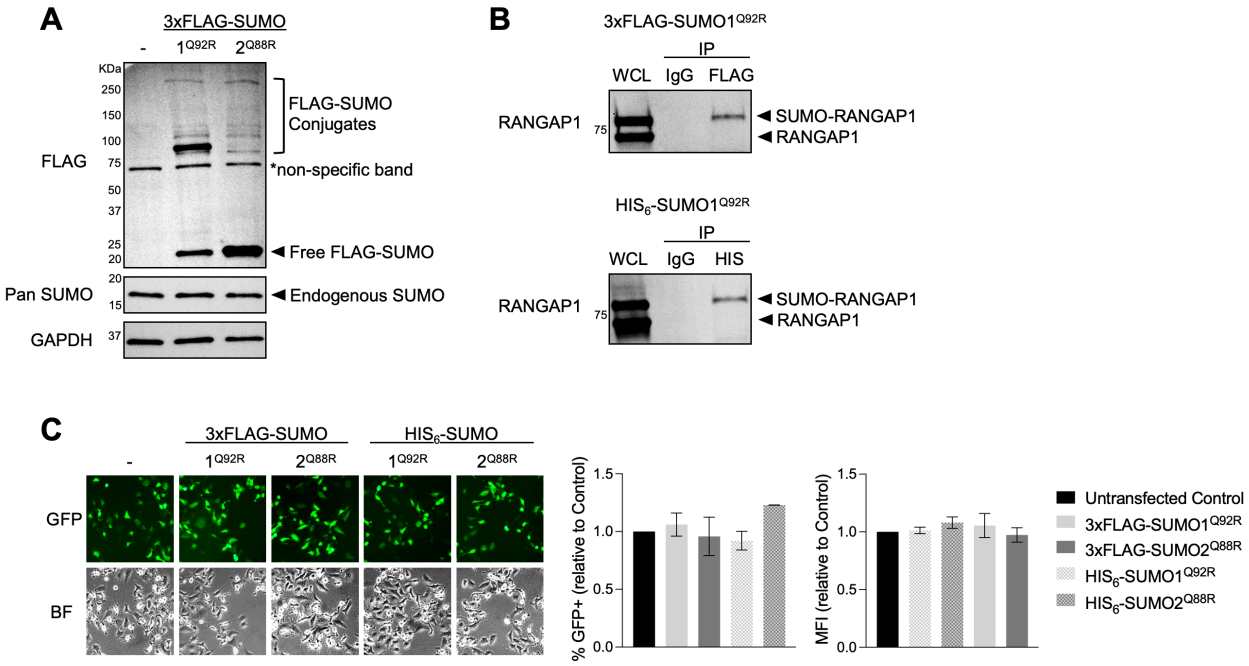

Supplemental Figure 1. Tagged SUMO mutants are conjugated to endogenous cellular proteins. (A) Western blot showing expression of free and conjugated forms of 3xFLAG-SUMO1^{Q92R} and 3xFLAG-SUMO2^{Q88R} in HeLa cells. Expression of endogenous wild-type SUMO is shown for comparison. "-" = Untransfected Control. **(B)** SUMO-modified RanGAP1 is detected following immunoprecipitation with a FLAG or HIS antibody in cells expressing 3xFLAG-SUMO1^{Q92R} or HIS$_6$-SUMO1^{Q92R}, respectively. Whole cell lysate (WCL) was used as input for IPs. Non-immune IgG = IP control. **(C)** Expression of exogenous SUMO does not interfere with HIV-1 infection. Cell lines were infected with equal volumes of viral supernatants containing VSV-G pseudotyped HIV-1 pNL4-3 deltaENV-EGFP reporter virus. %GFP+ cells and GFP mean fluorescence intensity (MFI) was assessed by flow cytometry at 24 hpi. "-" = Untransfected Control.

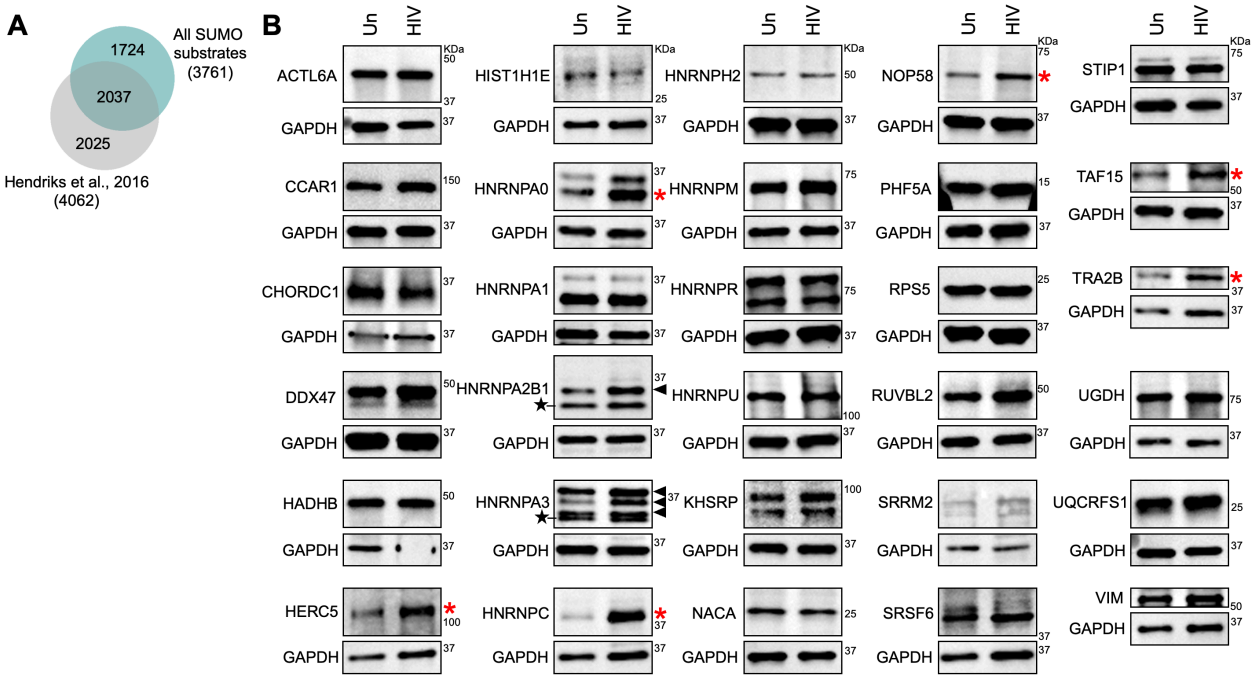

Supplemental Figure 2. Proteomic screen identifies proteins SUMOylated during HIV-1 infection. (A) Overlap between all SUMO substrates identified in this study versus the SUMOylated protein database described in Hendriks et al., 2016. **(B)** Western blots showing expression of select SUMO1 and SUMO2 substrates in HeLa cells left uninfected ("Un"), or infected with HIV-1. Samples were harvested for whole cell lysate preparation at 24 hpi. Arrows indicate SUMO-modified forms of HNRNPA2B1 and HNRNPA3 easily visible on a crude lysate. Stars indicate unmodified forms of these two proteins. Proteins that were increased in total abundance following HIV-1 infection are indicated with red asterisks.

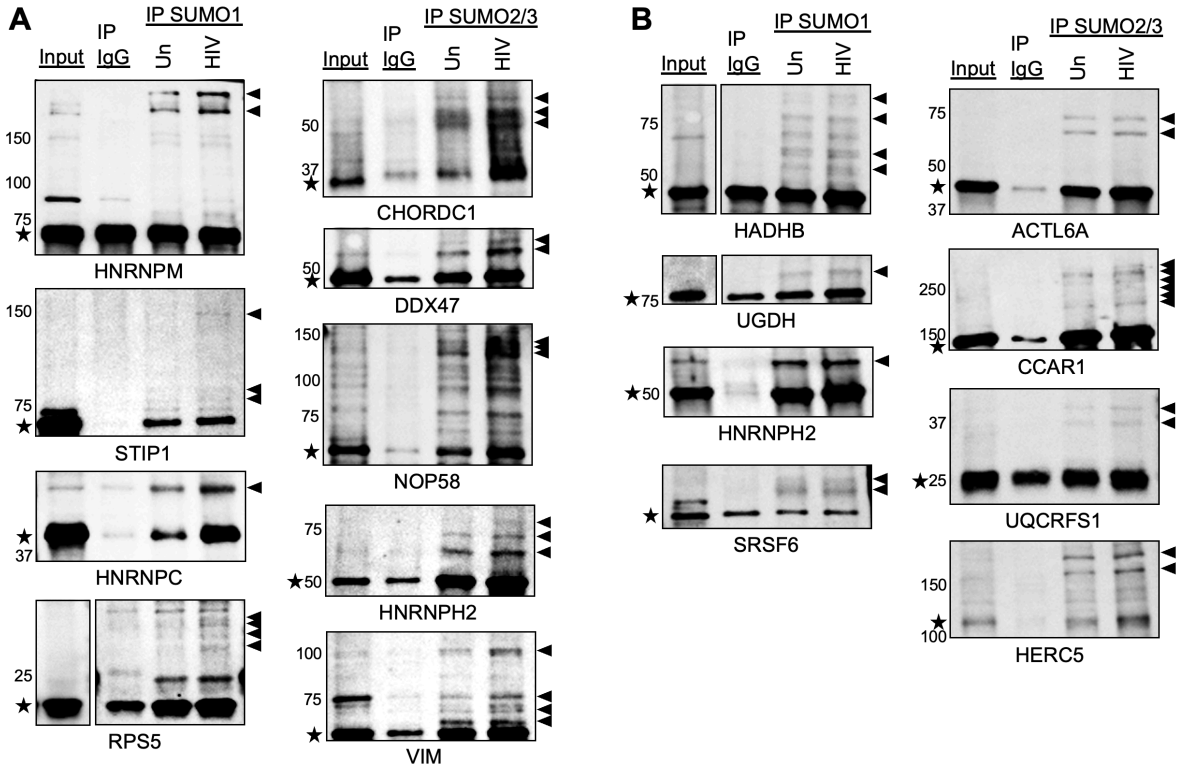

Supplemental Figure 3. Verification of additional HIV-1 induced SUMO targets. (A, B) Western blot analysis of SUMO1- or SUMO2/3-enriched samples from HIV-1-infected cells (”HIV”) versus uninfected controls (“Un”). SUMO-conjugates were immunoprecipitated using anti-SUMO1 or SUMO2/3 antibodies at 24 hpi as described in Figure 2, and samples were analyzed by western blot for the additional candidate substrates indicated below each blot. Stars indicate unmodified proteins. Arrows indicate SUMO-conjugated proteins. Crude lysate from HIV-1-infected cells was used as input for IPs. Input is 5% of protein loaded in IPs. Non-immune IgG = IP control.

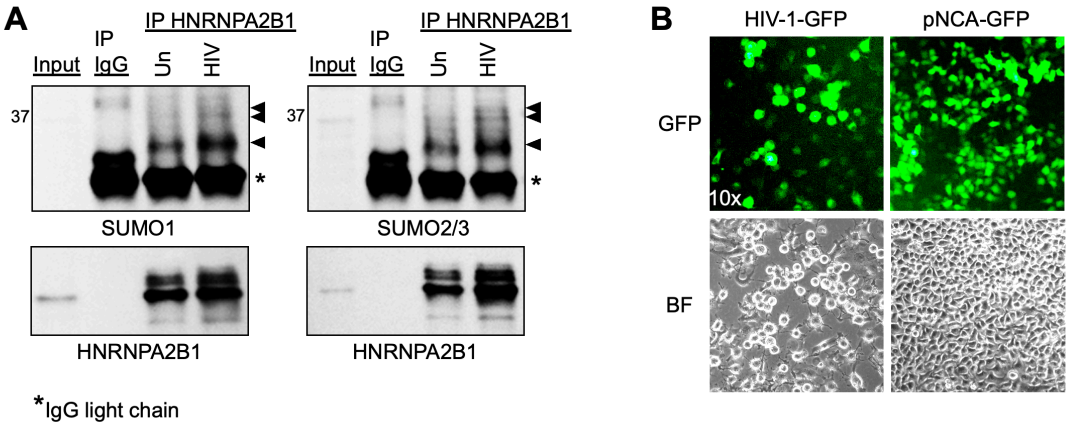

Supplemental Figure 4. Validation of HIV-1-induced hnRNPA2B1 SUMOylation. (A) Western blot analysis of HNRNPA2B1-enriched samples for SUMO1 and SUMO2/3 conjugation. HNRNPA2B1 was immunoprecipated from uninfected control ("Un") versus HIV-1-infected cells at 24 hpi., and samples were analyzed by western blot with anti-SUMO1 or SUMO2/3 antibodies. Arrows indicate SUMO-conjugated proteins. Asterisks indicate IgG light chain. Crude lysate from HIV-1-infected cells was used as input for IPs, where input was 5% of protein loaded in IPs. Non-immune IgG = IP control. **(B)** Representative images showing GFP expression in HeLa cells infected with VSV-G pseudotyped HIV-1 GFP versus MMLV reporter pNCA-GFP. Cells are shown at 48 hpi.

A

Final acceptor use	Control	A2B1-KD	A3-KD
A1	18.99	14.13	24.26
A2	5.6	8.98	4.7
A3	12.75	21.45	16.88
A4	18.43	16.14	12.13
A5	44.22	39.31	42.03

Control: A5>A1>A4>A3>A2
A2B1-KD: A5>A3>A4>A1>A2
A3-KD: A5>A1>A3>A4>A2

B

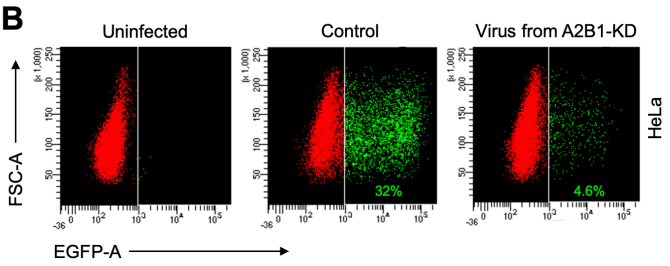

Supplemental Figure 5. Effect of HNRNP A2B1 and A3 knockdown on HIV-1 splicing and virion production. (A) Table showing average percent of spliced transcripts utilizing A1 through A5 initial and final splice acceptors in Control vs. A2B1- and A3-KD samples. The order of splice acceptor use, from most to least common, is listed for each sample. **(B)** Flow cytometry measuring GFP expression in HeLa cells infected with HIV-1-GFP virus produced by Control versus A2B1-KD 293T cells. GFP expression was measured at 24 hpi. Shown are representative images of three independent experiments.